ATTOSECOND HIGH HARMONIC PULSES: GENERATION AND TEMPORAL CHARACTERIZATION*

CHANG HEE NAM AND KYUNG TAEC KIM

Department of Physics and Coherent X-ray Research Center,
Korea Advanced Institute of Science and Technology (KAIST), Daejeon 305-701, Korea

A method to obtain near transform-limited attosecond harmonic pulses is presented along with techniques to characterize attosecond pulses, especially complete temporal reconstruction of attosecond pulses based on the frequency-resolved optical gating algorithm.

1. Introduction

Atoms driven by intense femtosecond laser pulse emit high harmonics in the xuv/soft x-ray wavelength region [1]. The high harmonic light source can provide an attosecond pulse train or a single attosecond pulse when properly controlled [2]. Because of its short duration, it is a valuable tool not only for the study of the ultrafast phenomena but also for understanding high harmonic processes in atom and molecules [3, 4].

The attosecond pulses obtained from high harmonic generation (HHG) contain a complex chirp structure [5, 6]. In single-atom calculations, the attosecond pulses, originating from the short quantum paths formed in the leading edge of the laser pulse, are positively chirped, resulting in longer pulse duration than that of the transform-limited pulse [5]. Since the positive chirp in the time domain corresponds to the positive second-order dispersion in the spectral domain, it can be compressed by passing through a material having negative group delay dispersion (GDD). Some x-ray filter materials have such negative GDD, and it has been shown that single sub-50-as pulses can be generated from neon atoms by using 700-nm-thick Sn filter by Kim et al. [5]. Experimentally 170 attosecond pulses were generated from Ar harmonics by using a 600-nm-thick Al filter by Martens et *al.* [7]. Since the material for the attosecond pulse compression need not to be a solid material, a gaseous medium

---

* This research was supported by the Ministry of Science and Technology of Korea through the Creative Research Initiative Program.

also can be applied. In fact, some rare gases, commonly used for the harmonic generation such as Xe, Ar, and Kr, have such negative GDD spectral region. When these gases are used for harmonic generation, the pulse compression may occur during harmonic generation without using an additional material.

Temporal characterization of attosecond pulses is still challenging task since efficient nonlinear material for two photon processes is difficult to realize in the xuv wavelength region. Autocorrelation techniques, widely used for the characterization of femtosecond pulses, can be applied only to limited cases of low-order harmonic pulses [8]. Cross correlation techniques, based on the photoionization by high harmonic and femtosecond laser pulses acting simultaneously, are thus valuable for the characterization of attosecond harmonic pulses [9, 10].

In this proceeding, a method to generate near transform-limited attosecond harmonic pulses is presented along with techniques to characterize attosecond pulses. The reconstruction of attosecond beating by interference of two-photon transition (RABITT) technique [9] is used for the chirp characterization and the estimation of pulse duration. For the full temporal characterization of attosecond pulses, the frequency-resolved optical gating for complete reconstruction of attosecond bursts (FROG CRAB) technique is also reported [10].

2. Temporal characterization of transform-limited attosecond pulses using RABITT

For the temporal characterization of complex harmonic pulses, one needs to precisely determine the spectral phase and amplitude of the harmonic pulses. In the RABITT method, the photoelectron spectra obtained from attosecond harmonic pulses with probe laser pulses are used for the reconstruction [9]. The photoelectron spectra show sidebands due to the interference of the electron wave packet ionized by two-photon transition. The sidebands are modulated with the time delay between harmonics and the laser. The phase information of the attosecond harmonic pulses can be found from the side band modulation:

$$A\cos\left(2\omega_0\tau+\Delta\varphi_q\right). \tag{1}$$

Here, A is the amplitude of the modulation, ω_0 is the laser frequency, τ is the time delay between harmonics and the laser, $\Delta\varphi_q$ is the phase difference of the $(q+1)^{th}$ and the $(q-1)^{th}$ harmonics. The spectral amplitude information can be found in the photoelectron spectrum without the laser field. The reconstruction of the attosecond harmonic pulses is possible from the phase and amplitude information.

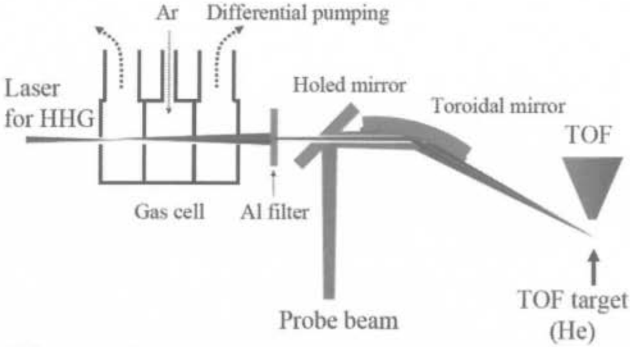

Figure 1. Schematics of the experiment setup. (TOF: time-of-flight electron spectrometer)

A 1-kHz Ti:sapphire laser, generating pulses of 30-fs duration, was used to obtain high harmonics, as shown in Fig. 1. The laser beam was split into two parts by a beam splitter. The first beam was focused into the middle gas cell for HHG. The second beam was used as a probe laser beam. After harmonic generation, the transmitted laser beam was blocked by a 200-nm aluminum filter to completely eliminate the laser light. The harmonic and the probe beams were combined using a mirror having a hole in the center and both beams were then focused together, using a gold-coated toroidal mirror, into a time-of-flight photoelectron spectrometer.

For the RABITT measurements, the attosecond harmonic pulses were generated with 2.5×10^{14}W/cm^2 laser in 12-mm-long 40-torr argon gas cell. First, the spectral amplitude of harmonics was obtained from the photoelectron spectrum of helium gas without using the probe beam. The photoelectron distribution was measured from 17th to 41st harmonic orders. In this case, the lower harmonics were severely absorbed (filtered) and the intrinsic positive chirp was compensated by the negative group delay dispersion of the argon medium itself. From the RABITT measurements, temporal profiles of attosecond harmonic pulses were reconstructed, as shown in Fig. 2. The full width at half maximum (FWHM) of the attosecond harmonic pulse was 206 as, very close to the transform-limited pulse width of 200 as.

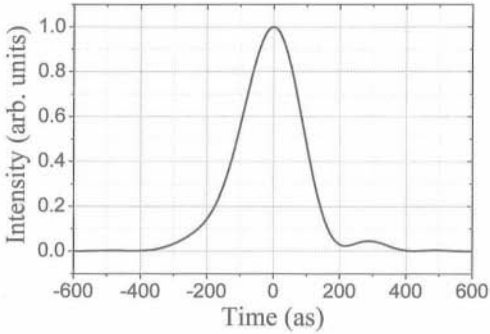

Figure 2. Reconstructed self-compressed attosecond harmonic pulses using RABITT technique.

3. Complete temporal characterization of attosecond harmonic pulses

The FROG CRAB method is an improved version of the RABITT technique, in which a 2-dimensional phase retrieval algorithm is used for the reconstruction. In the RABITT technique, each harmonic is assumed to be a plain wave [10]. Due to this assumption, it cannot be used for the reconstruction of the single attosecond pulse, having continuum spectrum. Also, the reconstruction result is always infinite pulse train, providing only averaged temporal characteristics of a real pulse train. As a consequence the chirp information of each harmonic is not available.

The FROG CRAB, on the other hand, has no such drawback, allowing the complete temporal information of attosecond pulses. For example, we can look into such issues as the duration and chirp structure of individual pulses in the attosecond pulse train and the harmonic frequency change in time with respect to harmonic order. This kind of information can be clarified from the FROG CRAB analysis.

In this technique, the photoelectron spectra obtained by applying harmonic and laser pulses together with time delay τ can be represented by

$$S(\omega,\tau)=\left|\int_{-\infty}^{+\infty} dt\; G(t)\,E_X(t-\tau)\,e^{i\omega t}\right|^2. \tag{2}$$

Here $\mathbf{E}_X(t)$ is the harmonic electric field to be measured and G(t) is the phase gate function, defined by

$$G(t)=\exp\left[i\int_t^{+\infty} dt'\;\left\{\mathbf{v}\cdot\mathbf{A}(t')+\mathbf{A}^2(t')/2\right\}\right], \tag{3}$$

where $\mathbf{v}$ is electron velocity and $\mathbf{A}(t)$ is the vector potential of femtosecond laser field. Since Eq. (1) is the spectrogram expressed in frequency and time delay, a conventional FROG inversion algorithm, such as the principal component generalized projection algorithm (PCGPA), may be used to reconstruct attosecond harmonic pulses [11]. Consequently, one can retrieve the harmonic electric field.

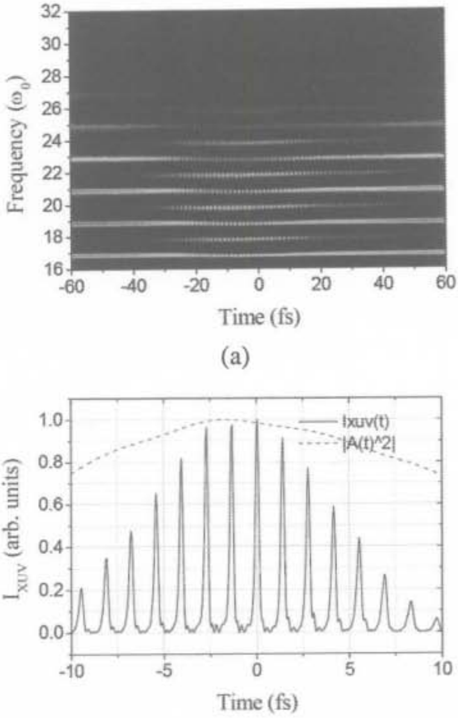

(a)

(b)

Figure 3. (a) Photoelectron spectra obtained from 20-torr argon with the probe laser beam. (b) The reconstruction of the attosecond harmonic pulses using FROG CRAB technique.

FROG CRAB measurements were carried out using the same experimental setup as shown in Fig. 1, but with the different harmonic conditions due to the poor energy resolution of the spectrometer at the high energy region. The attosecond harmonic pulses were generated in a 6-mm-long 25-torr argon gas cell up to the 31st harmonic order. In this case, the photoelectron spectra were obtained for the full range where harmonic pulses and probe pulses were overlapped, as shown in Fig. 3(a). The temporal reconstruction of the harmonic pulse, with orders higher than 17th that generate photoelectrons in He, was performed using the PCGPA algorithm. Figure 3(b) shows the reconstructed temporal profile of the harmonic pulse. The envelope width of the pulse train is 11 fs and the width of the attosecond pulse at the center of the train is 230 as. In this case, the intrinsic attosecond chirp at the center of the train is estimated to be 1.4×10^{-32} s^2, and the harmonic chirp of the 17th order is -2.3×10^{-28} s^2. Since the PCGPA is a blind FROG technique, not only the harmonic pulse, but also the laser field information is available. By comparing both fields, one will be able to obtain the information on ionization dynamics during the high order harmonic generation processes.

4. Conclusion

We have demonstrated self-compressed attosecond pulse generation with the pulse duration of 206 as, very close to the transform-limited value of 200 as. For the full temporal characterization of attosecond harmonic pulses, the FROG CRAB technique has been demonstrated. The attosecond pulses of 11-fs envelope width and 230-as pulse width at the center of the attosecond pulse train were measured.

References

1. M. Hentschel et al., Nature **414**, 509 (2001).
2. Ph. Antoine, A. L'Huillier, and M. Lewenstein, Phys. Rev. Lett. **77**, 1234 (1996).
3. T. Kanai, S. Minemoto, and H. Sakai, Nature **435**, 470–474 (2005).
4. R. Kienberger et al., Nature **427**, 817 (2004).
5. K. T. Kim, C. M. Kim, M.-G. Baik, G. Umesh, and C. H. Nam, Phys. Rev. A **69**, 051805(R) (2004).
6. H. J. Shin, D. G. Lee, Y. H. Cha, K. H. Hong, and C. H. Nam, Phy. Rev. Lett. **83**, 2544 (1999).
7. R. Lopez-Martens et al., Phys. Rev. Lett. **94**, 033001 (2005).
8. T. Sekikawa, A. Kosuge, T. Kanai and S. Watanabe, Nature **432**, 605 (2004).
9. P. M. Paul, E. S. Toma, P. Breger, G. Mullot, F. Augé, Ph. Balcou, H. G. Muller, and P. Agostini, Science **292**, 1689 (2001).
10. Y. Mairesse and F. Quéré, Phys. Rev. A **71**, 011401(R) (2005).
11. D. J. Kane, IEEE J. Quant. Elec. **35**, 421 (1999).